ACS SENSORS

pubs.acs.org/acssensors

Article

Nanoparticle-Based Liquid–Liquid Extraction for the Determination of Metal Ions

Tyler Z. Sodia, Alexa A. David, Ashley P. Chesney, Juliana N. Perri, Gwendolyn E. Gutierrez, Cecilia M. Nepple, Sydney M. Isbell, and Kevin J. Cash*

Cite This: *ACS Sens.* 2021, 6, 4408–4416

Read Online

ACCESS | Metrics & More | Article Recommendations | Supporting Information

ABSTRACT: Traditional liquid phase extraction techniques that use optically responsive ligands provide benefits that enable cost-efficient and rapid measurements. However, these approaches have limitations in their excessive use of organic solvents and multistep procedures. Here, we developed a simple, nanoscale extraction approach by replacing the macroscopic organic phase with hydrophobic polymeric nanoparticles that are dispersed in an aqueous feed. The concentration of analytes in polymeric nanoparticle suspensions is governed by similar partition principles to liquid–liquid phase extraction techniques. By encasing optically responsive metal ligands inside polymeric nanoparticles, we introduce a one-step metal quantification assay based on traditional two-phase extraction methodologies. As an initial proof of concept, we encapsulated bathophenanthroline (BP) inside the particles to extract then quantify Fe^{2+} with colorimetry in a dissolved supplement tablet and creek water. These Fe^{2+} nanosensors are sensitive and selective and report out with fluorescence by adding a fluorophore (DiO) into the particle core. To show that this new rapid extraction assay is not exclusive to measuring Fe^{2+}, we replaced BP with either 8-hydroxyquinoline or bathocuproine to measure Al^{3+} or Cu^{+}, respectively, in water samples. Utilizing this nanoscale extraction approach will allow users to rapidly quantify metals of interest without the drawbacks of larger-scale phase extraction approaches while also allowing for the expansion of phase extraction methodologies into areas of biological research.

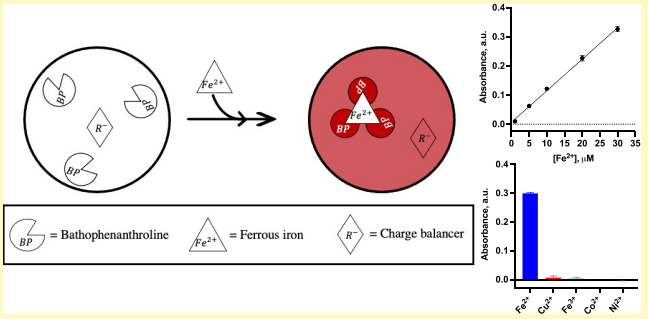

KEYWORDS: *metal determination, extraction, nanoparticles, nanosensors, optical probes*

Quantifying metals is an ongoing scientific problem that has implications in a wide range of disciplines.[1−4] Traditional measurement techniques that use large-scale equipment (e.g., atomic absorption, X-ray absorbance or fluorescence, and inductively coupled plasma-mass spectrometry) have benefits such as high sensitivity, identification of oxidation states, and multiple element determination. However, there are disadvantages such as complicated operations, expensive equipment and reagents, and time-intensive sample preparation. For researchers that prefer a technique with minimal sample preparation and a simple, sensitive quantification, these techniques are impractical. Alternatively, there are small-scale analytical techniques that can be applied to a wide range of applications and are easier to integrate into routine experiments in the laboratory without the need for expertise.[5,6]

A typical, simpler approach for metal quantification uses liquid–liquid extraction (LLE) procedures.[7] These assays function on the basis of metal–ligand complex formation and its relative solubility in one of two immiscible liquids, typically an aqueous phase and an organic phase. While the metal salt resides in the aqueous phase, the organic phase consists of an optically responsive, hydrophobic ligand that binds to the metal in the hydrophobic phase, stabilizes it, and changes the optical properties to enable detection. While somewhat easy to operate, these techniques can require large amounts of organic solvents, which can be toxic and hard to dispose of. Further advances like solid phase extraction (SPE), cloud-point extraction, or dispersive liquid–liquid microextraction (among others) have been developed to quantify analytes while using significantly smaller volumes of harmful solvents;[8] however, these techniques can require expensive equipment, extensive procedures, and a need for additional expertise.

Classic examples of LLE and subsequent metal quantification originate from assays involving probes related to 2,2′-bipyridine.[9,10] These complexes generally absorb in the visible wavelength range due to their metal-to-ligand charge transfer

Received: August 19, 2021
Accepted: November 9, 2021
Published: November 18, 2021

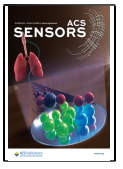

band and can be quantified using UV−vis spectroscopy.[9] Building on this premise, related species that have selectivity for Fe^{2+} have gained popularity.[11−13] For example, 4,7-diphenyl-1,10-phenanthroline (bathophenanthroline, BP) has enabled sensitive detection of Fe^{2+} down to low micromolar concentrations even in the presence of Fe^{3+} and other potential competing analytes.[14,15] While widely accepted and seemingly straightforward, this technique has required acid digestion for sample pretreatment and $Fe(BP)_3^{2+}$ extraction into a bulk organic phase, resulting in the same LLE issues stated above. Using the same ligand, some have performed SPE to measure Fe^{2+},[16] but these methods tend to have poor response times.[17]

Polymeric nanosensors (PNS) are an analytical tool that gives the user the ability to measure ions or small analytes by encasing optically responsive sensing components into a nanoscale hydrophobic polymer matrix. Most of the PNS are plasticized polymer nanoparticles solubilized by a surfactant coating and dispersed in an aqueous phase. There are many sensing mechanisms for PNS discussed in fundamental reviews of the field,[17,18] and more recent mechanistic developments are discussed elsewhere.[19−22] Conventionally, the target ion is extracted from the aqueous phase and stabilized in the hydrophobic particle core by the recognition group. Upon extraction, the luminescent output of the nanoparticle is altered. This can be a result of altering the protonation degree of a pH-sensitive dye, displacing a solvatochromic dye into the aqueous phase, or the quenching of either the fluorescence or phosphorescence of a particular transducer inside the particle.[19−22] Polymeric nanosensors have been used to measure a wide range of analytes in both biological (*in vitro* and *in vivo*) and chemical systems and have shown advantageous character over their electrode and bulk membrane counterparts.[17]

One example of nanoparticle-based measurement systems is Bakker and coworkers' exploitation of the technology to make more sensitive and selective complexometric titration reagents to measure alkali, alkaline earth metals, and the anions NO_3^- and ClO_4^-.[23−25] The reagents had optical readouts by encapsulating solvatochromic dyes or chromoionophores, which significantly simplified the identification of the endpoint in their titrations.[24,26] The use of nanoemulsions in this regime resulted in heterogeneous complexometric reagents that are more sensitive than the homogeneous-based methods and allow for highly selective hydrophobic ligands to be utilized in titrimetry. Creating heterogeneous complexometric reagents further illuminated the potential for PNS to be used in a wide range of analytical analyses.

The extraction process of classic LLE and the sensing mechanism for PNS follow similar principles, with partitioning of the analyte between two immiscible phases and optical changes in a reporter group. Accordingly, we hypothesized that the encapsulation of optically responsive ligands into polymer nanoparticles would enable a rapid quantification of metals of interest without the drawbacks of traditional LLE. While nanoemulsions have been utilized as complexometric reagents, our nanoparticle approach has shown that ligands that are typically dissolved in bulk organic phases can be encapsulated into polymeric nanoparticles while maintaining their metal-sensing functionality. This approach enables easier analytical procedures and allows for adaptations of general LLE approaches to novel biological applications where LLE is not feasible. By utilizing the components of PNS as an extraction matrix, metals that are usually quantified through bulk liquid phase extraction methods can instead be measured with smaller volumes of harmful reagents and much higher throughput. In this manuscript, we describe the combination of optically responsive ligands traditionally used for LLE and PNS as a nanoparticle extraction method for quantifying metals in water samples (demonstrated with Fe^{2+}, Al^{3+}, and Cu^+) toward a general platform for the adaptation of LLE-based methods.

EXPERIMENTAL SECTION

Materials. Polyvinyl chloride (PVC), bis ethylhexyl sebacate (DOS), bathophenanthroline (BP), 8-hydroxyquinoline (8HQ), bathocuproine (BC), tetrahydrofuran (THF), dichloromethane (DCM), sodium tetrakis-[3,5-bis(trifluoromethyl)phenyl]borate (NaBARF; Selectophore), sodium acetate, glacial acetic acid, Dulbecco's phosphate-buffered saline (PBS), ammonium iron(II) sulfate hexahydrate, iron(III) chloride, cobalt(II) sulfate hydrate, copper(II) sulfate, nickel(II) sulfate, magnesium sulfate, and thioglycolic acid were all purchased from Sigma-Aldrich (St. Louis, MI, USA). 3,3′-Dioctadecyloxacarbocyanine perchlorate (DiO; Invitrogen) and 1,1′-dioctadecyl-3,3,3′,3′-tetramethylindodicarbocyanine, 4-chlorobenzenesulfonate salt (DiD; Invitrogen) were purchased from Thermo Fisher Scientific (Waltham, MA, USA). Microdialysis hollow fibers (13 kDa cutoff) were purchased from Spectrum Laboratories, Repligen (Waltham, MA, USA). Ferrous sulfate supplement tablets were purchased from Signature Care. Creek water was obtained from Clear Creek in Golden, CO, USA on February 21, 2021.

Fabrication. The procedure for all preparticle mixtures started by placing polyvinyl chloride (PVC) into 2 mL glass vials with Teflon-lined caps. DOS was added to the PVC and set aside. The ionic additive (NaBARF) was brought into 250 μL of THF and added to the PVC vial. This vial was vortexed until the PVC was fully dissolved. The ligand, which was dissolved in DCM, was added to the PVC vial and vortexed for 45 s. The fluorescent Fe^{2+} NS required that DiO (also dissolved in DCM) be added at the same point as the ligand. All preparticle mixtures were stored in a refrigerator at 4 °C. For the mass of each component, see Table S1.

All NS batches were made with the same protocol, following a similar procedure to Dubach *et al.*[27] Two milligrams of the PEG-lipid was put into a 4-dram scintillation vial. While the PEG-lipid is used for the solubilization of these nanoparticle sensors, other surfactants have been used in similar nanosensors (such as triblock copolymers).[28,29] Acetate buffer (pH 4.6 unless stated otherwise) was added to the scintillation vial at a volume of 5 mL and then sonicated with a probe tip sonicator (Branson Digital Sonifier 450; Branson Ultrasonics Corporation, Danbury, CT) for 30 s at 20% of its maximum power. A total of 100 μL of the preparticle mixture was added to the acetate solution and sonicated for 3 min under 20% maximum power. After sonication, the excess polymer was removed with a 0.8 μm filter (Pall Corporation, Port Washington, NY, USA), and the filtrate was stored in a 1.5-dram screw cap glass vial at room temperature in the dark.

Nanosensor Characterization. The calibration curves of the NS were obtained by loading 100 μL of analyte standard dilutions (in acetate buffer) and 100 μL of NS solution into the wells of a Nunc MicroWell 96-well optical-bottom plate (Nalgene Nunc International, Roskilde, Denmark). This yielded a final volume of 200 μL in each well and concentrations ranging from 0.5 to 150 μM Fe^{2+}, 0.5 to 100 μM Cu^+, or 1 μM to 1 mM Al^{3+} for each respective NS calibration. The selectivity of the Fe^{2+} NS was determined with the separate-solution method against Cu^{2+}, Fe^{3+}, Co^{2+}, and Ni^{2+} dilutions. The Cu^+ and Al^{3+} NS selectivities were obtained by two-point, separate-solution calibrations of each competing analyte at 100 μM. Each calibration was obtained in triplicate using a Synergy H1 microplate reader with absorbance readings at 533 and 478 nm or a fluorescence endpoint at 505 nm for Fe^{2+}, Cu^+, or Al^{3+}, respectively.

The Fe^{2+} NS fluorescence readout was obtained by exciting each sample at 450 nm and measuring fluorescence of DiO at 501 nm. All standards were made new for each calibration to limit errors due to

https://doi.org/10.1021/acssensors.1c01780
ACS Sens. 2021, 6, 4408−4416

analyte oxidation. To obtain the Cu^{+} solution, 0.2% thioglycolic acid was added to Cu(II)SO_4 (1:10 v/v). Further standard dilutions were made from this stock.

All NS calibrations were fit to either a simple linear regression or a 4-parameter logistic equation with GraphPad Prism 9.1.2 software (San Diego, CA, USA). The statistical analyses for all calibrations were also done in GraphPad Prism 9. The limits of detection were calculated according to ref 30.

The reversibility of the Fe^{2+} NS was tested using the procedure by Ferris *et al.*, with some variation.[22] Briefly, the Fe^{2+} NS were concentrated to a 10× stock, put into a hollow fiber microdialysis tube (MWCO, 13 kDa; Spectrum Laboratories), and sealed at each end and then secured into an untreated 6-well culture plate with epoxy. After the epoxy dried, acetate buffer was put into the same well and conditioned for 3 h. Then, the initial absorbance (533 nm) and fluorescence (λ = 450/501) reading was taken on the Synergy H1 microplate reader using the area scan settings (11 × 5, 1600 × 1600 μm spacing). The acetate buffer was removed, and the well was rinsed before a dilution of 150 μM Fe^{2+} was put into the well and incubated for 30 min. After incubation, a measurement was taken with the same settings, and the Fe^{2+} dilution was removed before another rinse and addition of acetate-buffered solution. This cycle was repeated twice in triplicate.

The Fe^{2+} NS functional lifetime was measured by calibrating the fluorescence response according to the procedure on days 0, 2, 4, and 7.

Analysis of Real Samples. The reliability of the measurements was tested with the Fe^{2+} NS against a ferrous sulfate supplement tablet. One tablet (205 mg of anhydrous ferrous sulfate) was dissolved in half a liter of acetate buffer and filtered with a 0.8 μm PES membrane syringe filter. A series of two-fold dilutions were made until the theoretical concentration (calculated by the dilution factor and the 205 mg tablets) was within the NS linear range. These dilutions were mixed with NS into the wells of a 96-well plate, and an absorbance value at 533 nm was obtained with the Synergy H1 microplate reader. With the absorbance values of the supplement dilutions, the respective concentrations were back calculated with the regression line of the standard curve. Taking the calculated concentrations and dividing them by their dilution factor (stock = 1, dilution 1 = 0.5, dilution 2 = 0.25, etc.) allowed us to calculate the concentration of ferrous sulfate in the stock solution. We also attempted to measure Fe^{2+} in creek water with the standard addition and external standard method.[31] The accuracy of the Fe^{2+} NS measurements was confirmed by a comparison to a Hanna colorimeter—Checker HC (Woonsocket, Rhode Island, USA)—that is used for selectively measuring total iron.

RESULTS

Our Fe^{2+} nanosensors (Fe^{2+} NS) incorporate bathophenanthroline (BP, log P = 3.37[32]) as the recognition agent and reporter for Fe^{2+}. Instead of extracting Fe^{2+} from the aqueous to the organic liquid phase, our approach uses BP to extract Fe^{2+} into a polymer nanoparticle phase with a 3:1 BP:Fe^{2+} ratio (Scheme 1).

In the absence of Fe^{2+}, BP does not absorb light from 300 to 700 nm. Increasing Fe^{2+} in the system results in a BP-mediated Fe^{2+} extraction and stabilization in the polymer phase, causing an extensive increase in absorbance with a peak at 533 nm (Figure 1). Using these data, a calibration curve was obtained using a set of standards ranging from 0 to 150 μM ferrous sulfate. The Fe^{2+} NS have a linear range from 1 to 30 μM (R^2 = 0.994) and a limit of detection (LOD) of 0.8 μM (Figure S2). This linear range is sufficient for immediate implementation into a variety of applications like environmental water testing[33,34] and serum-based diagnostics[35] (potentially requiring additional sample preparation to release transferrin-bound iron).

Scheme 1. Sensing Mechanism of the Fe^{2+} Nanosensors[a]

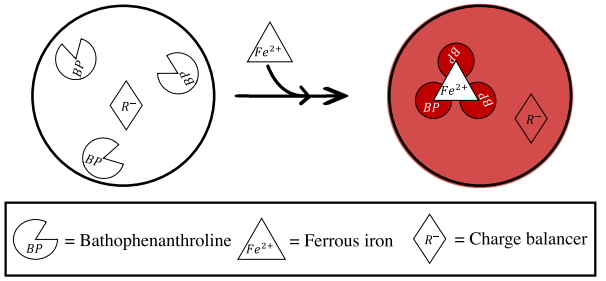

[a]Without Fe^{2+} in the system, the sample does not absorb light at 533 nm. BP selectively extracts Fe^{2+} into the polymer phase and undergoes a large increase in absorbance at 533 nm, creating a red sample.

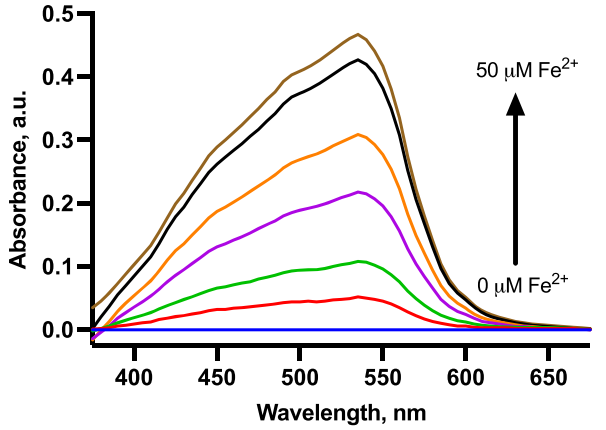

Figure 1. Increasing Fe^{2+} results in a large absorbance peak at 533 nm from the nanosensors. Linear and semilog calibration curves from this data are provided in Figure S2.

The sensor mechanism and the efficiency of BP incorporation into the nanoparticles were tested by centrifugal filtration and subsequent testing on the filtrates. No optical response was seen when adding 50 μM Fe^{2+} to the nanosensor filtrate, and minimal absorbance (533 nm) was observed in the filtrate of the nanosensors that already responded to 50 μM Fe^{2+} (Figure S1).

Before the analysis of a real sample, the Fe^{2+} NS selectivity was tested against Fe^{3+} chloride and Cu^{2+}, Co^{2+}, and Ni^{2+} sulfates. All resulting response curves for potentially interfering metals showed negligible changes in absorbance at 533 nm (Figure 2). Phenanthrolines have also been shown to chelate other metals and absorb light at some capacity at a range of wavelengths.[36] Absorbance spectra for the other metals are shown in Figure S3 and confirm no significant increase in absorbance between 300 and 700 nm.

Other BP-based assays have shown poor selectivity over Cu^{n+} species,[12] as phenanthroline and its derivatives can form a 2:1 cuprous complex, which has an absorption maximum at ~478 nm and is extractable into an organic phase.[37] Thus, more confirmation of the selectivity over Cu^{2+} and its impact on our Fe^{2+} calibrations was needed. According to the U.S. Agency for Toxic Substances and Disease Registry, the average amount of copper in river water is 0.16 μM.[38] Accordingly, we calibrated the Fe^{2+} NS to a new set of standard dilutions that were spiked with a range of relevant Cu^{2+} concentrations (0−5 μM). Figure S4 shows low Cu^{2+} interference on the Fe^{2+} response. The Fe^{2+} calibrations with spiked Cu^{2+} showed no

https://doi.org/10.1021/acssensors.1c01780
ACS Sens. 2021, 6, 4408−4416

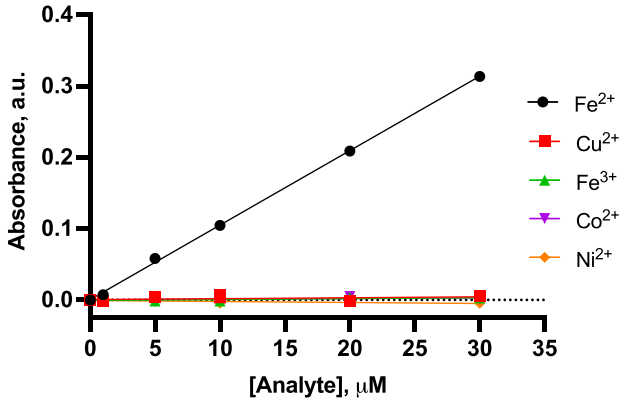

Figure 2. Calibration curves obtained with other transition metal standards show a negligible response at 533 nm deeming the sensors highly selective for Fe^{2+} over the other analytes. n = 3, and error bars are smaller than data points.

difference compared to the standards without Cu^{2+}. All calibrations held a good linear range between 1 and 30 μM.

After demonstrating Fe^{2+} NS selectivity, Fe^{2+} in a ferrous sulfate supplement tablet was measured. Dissolving the supplement tablet in 0.5 L of acetate buffer yielded a stock concentration of 2.7 mM. Measuring the two-fold dilutions that fell within the linear range of the assay resulted in a final calculated mass of 206 ± 8 mg of ferrous sulfate. A high correlation was obtained when comparing these measurements to those from a commercially available method for the determination of total iron (Figure 3). In addition to measuring Fe^{2+} in a supplement tablet, the sensors were also used to measure water collected from Clear Creek in Golden, Colorado with the standard addition method. Statistical analysis of the regressions from spiked, unknown samples and standards showed no difference between slopes, revealing negligible matrix effects in the sample (Figure S5). The

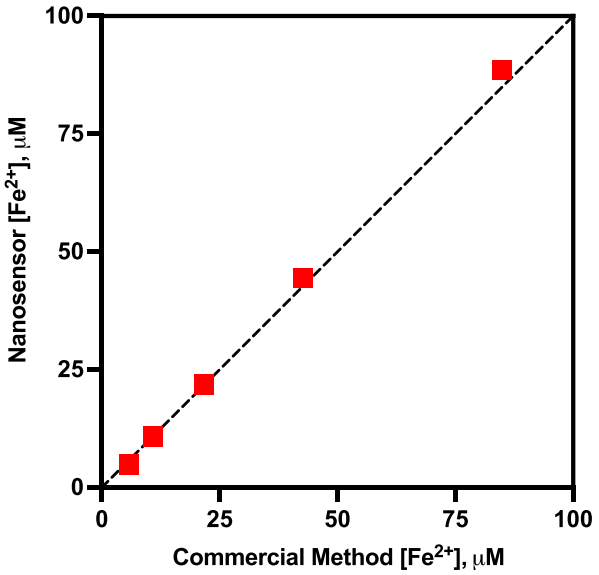

Figure 3. Measured iron concentrations from dilutions of a supplement sample obtained with the Fe^{2+} nanosensors (y-axis) highly correlate with those obtained with a standard commercial iron selective colorimeter (x-axis). The dashed line indicates a slope of 1 between the two methods. n = 3, and error bars are smaller than the data points.

method of external standards showed no measurable Fe^{2+} in the creek water, which was also confirmed with the Fe^{n+}-selective Hanna colorimeter.

Following prior work with a fluorescence gating mechanism,[21] we incorporated a fluorescent reporter, which is not sensitive to Fe^{2+} (DiO) into the particle core to exhibit the user-tunability of this approach to a broader set of applications. Due to the sufficient spectral overlap between the absorbance of $Fe(BP_3)^{2+}$ and the emission of DiO, the Fe^{2+} NS show a large turn-off response to increasing Fe^{2+} (Figure 4). These

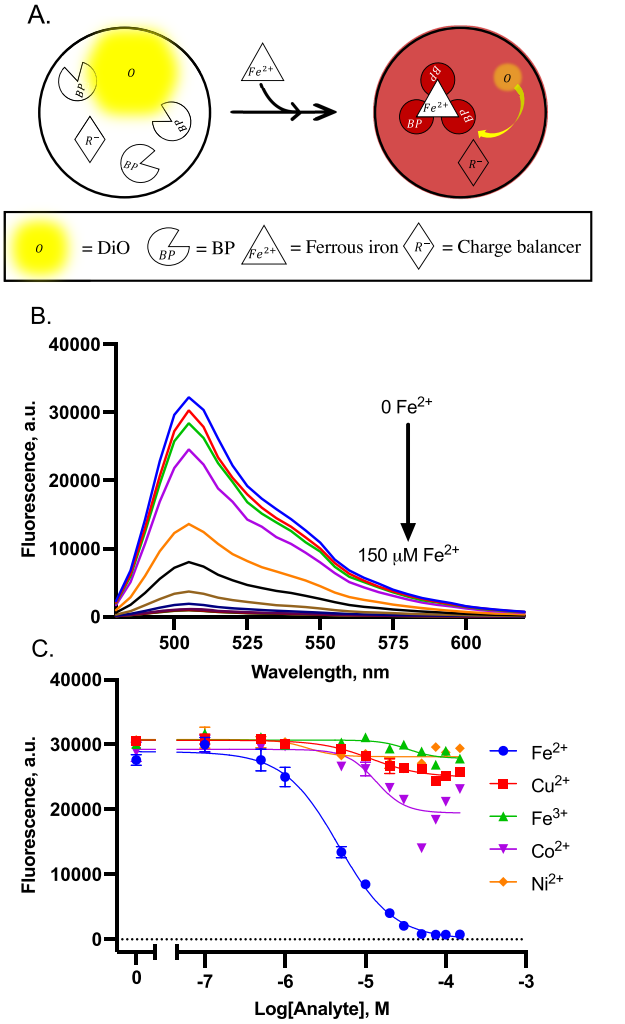

Figure 4. (A) Introducing a lipophilic fluorescent indicator (DiO, λ_{em} of 501 nm) into the colorimetric Fe^{2+} NS results in a fluorescence assay for Fe^{2+} determination. (B) Exposure to Fe^{2+} results in high absorbance at 533 nm, which sufficiently gates the DiO emission, causing a decrease in measured fluorescence. (C) Sensors are selective for Fe^{2+}. n = 3 for panels (B, error bars not shown) and (C).

calibrations resulted in a response midpoint of 2.1 μM (Figure 4C). In conjunction with the colorimetric responses shown in Figure 2, the fluorescence calibrations for the Fe^{2+} NS against the competing analytes show good selectivity (K_{ij} based on a 50% maximal potential signal change shows no response for off-target analytes due to minimal response) (Figure 4C). Moreover, the midpoint of the fluorescence response of these sensors is stable for at least 4 days (Figure S6). Due to the prevalence of fluorescence quenching by transition metals, including Fe^{2+},[39] controlling for the possibility that other

https://doi.org/10.1021/acssensors.1c01780
ACS Sens. 2021, 6, 4408−4416

targets would quench DiO was a necessity. Sensors without BP (which should not respond to Fe^{2+}) had no DiO response to increasing analyte concentrations (Figure S7).

At circumneutral pH (pH ~6−8), $Fe^{2+}_{(aq)}$ is not thermodynamically stable and is rapidly oxidized to Fe^{3+} in the presence of oxygen.[40] As BP is easily protonated at acidic pH, it was necessary to determine the impact of pH on the Fe^{2+} NS response. The response at 50 μM Fe^{2+} was measured at pH 3.6, 4.6, and 5.6 (Figure S8). Indeed, the sensor response at pH 3.6 was amplified relative to the signal at pH 5.6. Prior analyses of both colorimetric and fluorescent phenanthroline-based probes show an irreversible response to Fe^{2+}.[41] As expected, our approach is also irreversible (Figure S9).

To test how general our nanoparticle extraction is, we used the same approach with optically responsive ligands for both Al^{3+} and Cu^{+}. For sensing Al^{3+}, we used the responsive probe 8-hydroxyquinoline (8HQ, log P = 1.72[42]). 8HQ extracts and stabilizes the free Al^{3+} from the aqueous phase into the sensor core with a 3:1 stoichiometry.[43] Increasing Al^{3+} in the system enhances the fluorescence at 505 nm due to the formation of the $Al(8HQ)_3$ complex inside the particle. Using standard buffer solutions, the Al^{3+} NS show a linear range from 10 to 100 μM (Figure 5A). Al^{3+} is often leached into streams and other water bodies when the pH is below circumneutral.[44] The range of the Al^{3+} NS allows for application in the analysis of acid mine drainage or acid rain runoff where Al^{3+} can easily exceed 10 μM.[45] While 8HQ can chelate other metals, our selectivity tests (100 μM analyte) show that the Al^{3+} NS are selective (Figure 5A, inset). The spectra from the NS−analyte mixtures show no significant fluorescence peak from 300 to 800 nm (Figure S10).

The Cu^{+} NS response is mediated by a BP derivative, bathocuproine (BC, log P = 4.47[46]). Inside the particle, the $Cu(BC_2)^{+}$ undergoes metal-to-ligand charge transfer and increases absorbance with a peak at 478 nm in response to Cu^{+} (Figure S11). The calibration of these sensors with standard buffer sets resulted in a linear range between 1 and 20 μM (Figure 5B). The Cu^{+} sensors also showed good selectivity over other metals (Figure 5B, inset).

Similar to the Fe^{2+} NS, the characterization of the extraction mechanism and confirmation of sufficient ligand partition were done through centrifugal filtration and testing of the filtrate (Figure S1). Additionally, as expected, both the Al^{3+} and Cu^{+} NS responses were impacted by pH (Figure S8).

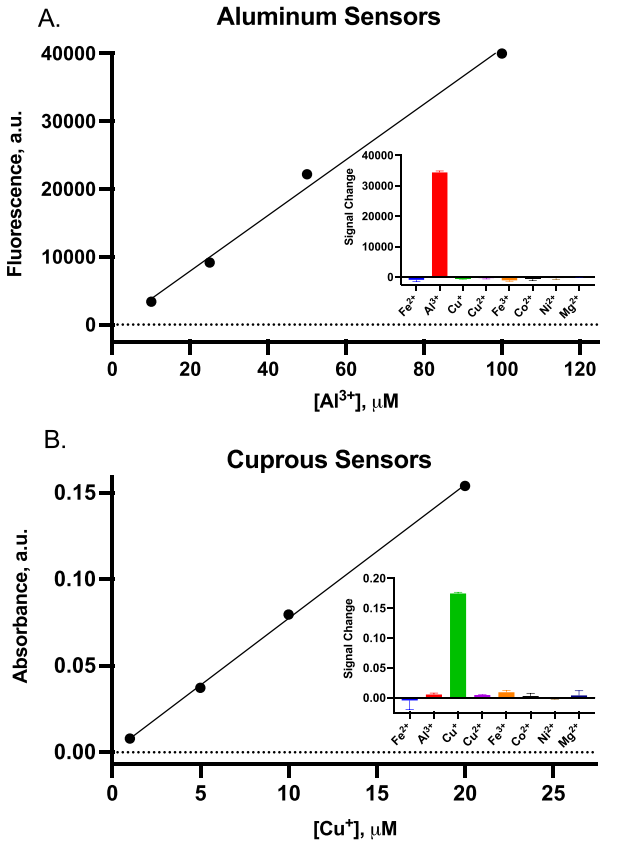

Figure 5. This approach is not exclusive to Fe^{2+} extraction and quantification. Using an optically responsive ligand (8HQ, λ_{em} = 505 nm) for Al^{3+} results in (A) sensitive and (A, inset) selective NS for Al^{3+} (R^2 = 0.9985). (B) Using BC, Cu^{+} NS show an increased absorbance at 478 nm (R^2 = 0.9989) and (inset) high selectivity for Cu^{+}. Calibrations are in standard buffer sets with n = 3. Where not visible, the error bars are smaller than data points.

DISCUSSION

The quantitation of metals is a challenge that has implications in medicine, microbiology, water chemistry, and geology.[1−4] Innovations upon demanding analytical procedures that allow for quick and high-throughput analysis are a necessity. Our nanoparticle extraction assay provides a platform that enables easy quantification of metals by adopting bulk phase extraction reagents and principles. The partition principles that govern the extraction of the analyte of interest are similar to those of traditional LLE.[47] Namely, the metal ion is poorly soluble inside the hydrophobic extraction phase without the stabilization by the selective ligand; with this component, the ion is stabilized in the particle, while the other analytes remain in the aqueous phase.

Others have used similar materials (plasticized PVC) for improved extraction methods of Fe^{2+}, Cu^{+}, and many other analytes into a polymer membrane instead of an organic liquid.[16,48] Alternative materials have also been used for solid phase extraction (SPE); Martínez *et al.* investigated the partition of the phenanthroline−Fe^{2+} complex in modified acrylamide hydrogels.[49] They determined the free Fe^{2+} concentrations in milk, providing a method for spectrophotometric measurement in opaque samples. Similar to some metal-selective bulk optode membranes,[50,51] these SPE approaches have resulted in a long response time (i.e., a t_{95} of 15−50 min[49,52]) when analyzing real samples due to their dependence on both diffusion of the ligand inside the matrix as well as mass transport of the small amount of the analyte in the aqueous phase.[17] For sensors with a polymeric foundation, transitioning from a planar surface to a nanoparticle dispersion has allowed for significantly lower response times due to a much larger surface area-to-volume ratio.[17] In this work, the response time is too fast to measure with our equipment and approach. We know that the sensor responds faster than the time it takes between sample preparation and sample measurement (~15 s), but the response time is likely closer to the ~ms regime as demonstrated with similar sensors.[53]

By adopting the structure from polymeric nanoparticle sensors (PNS), our extraction approach not only benefits from a faster response time but also adds the potential application in systems where LLE and its variations are not feasible. Nanoparticle sensors with this structure have been used to

https://doi.org/10.1021/acssensors.1c01780
ACS Sens. 2021, 6, 4408−4416

characterize complex biological systems such as clinically grown biofilms of *Pseudomonas aeruginosa*, eukaryotic intracellular environments, and animal models by probing for a range of diverse analytes.[53−55] A large factor to consider when applying analytical techniques to live models is the biocompatibility of the reagents used as well as the assay's procedure itself.[56] The reagents used in classic LLE and variations thereof are often toxic to live samples. For example, applying a large amount of an organic solvent to a live biological sample while using traditional LLE will quickly destroy the sample's integrity. Though liquid phase microextraction (LPME) methods decrease the solvent volume, biological samples still consist of highly complex matrices that may interfere with liquid−liquid phase interfacial tension, which can be detrimental to extraction efficiency.[57] As a result, many liquid extraction methods require pretreatment of the sample, a hindrance not required with PNS.

Another benefit of the PNS methodology is the ability to substitute the sensing components inside the particles when the analyte of interest changes.[17] Thus, the nanoparticles in this work can be used as an extraction phase for more than just one analyte, provided that there is a hydrophobic ligand that solubilizes inside the polymer matrix. We show in Figure 5 that this approach can be tailored to an analyte of interest depending on the ligand encased in the dispersed polymer phase while using the same structural materials with no additional steps.

Utilizing an optically responsive ligand resulted in sensors that coupled the recognition and transduction moieties inside the particle, though this is not mandatory. Other nanoparticle sensors have separated these elements by utilizing an optically inert ligand for extraction and quantification through ion exchange equilibrium with a pH-sensitive fluorescent dye[17,18] or by adding an additional optically responsive readout component into the particle.[20−22,58] Fluorescence gating mechanisms similar to our DiO approach would likely be infeasible in bulk liquid phase extractions due to the distance between the optically active groups, demonstrating an additional benefit to embracing nanoparticles for the extraction matrix.

The sensing approach that we use here is similar to the optical complexometric reagents that were introduced by Bakker and associates.[23−26] However, in their work, the recognition and transduction elements are distinct moieties; in this work, they are combined. While mechanistically simpler than the NS with distinct recognition and transduction components, there are drawbacks here such that the sensor response is less straightforward to adjust.

The addition of a ratiometric readout to fluorescent sensors allows for the quantitation of an analyte in a highly complex sample due to the multiwavelength measurement.[59] While this readout method is preferable, especially with complex matrices, the incorporation of additional fluorophores into the nanoparticle also adds potential complexity that may be hard to predict. Our approach does not avoid this complexity. The addition of DiD as a reference signal into our Fe^{2+} NS exhibited a favorable ratiometric (DiO/DiD) response to Fe^{2+} but a large, unwanted increase in the presence of Cu^{2+} (Figure S12). Future works will focus on this off-target interaction. The ratiometric Fe^{2+} NS were still selective over metals other than Cu^{2+}, which may still prove to be useful in some settings. Nevertheless, the other two readout approaches (501 nm emission and 533 nm absorption) provided high selectivity over analytes that may compete with BP's binding moiety (Figures 2 and 4C).

Our NS are not ratiometric; thus, the sensor response is impacted by sensor concentration. Specifically, by diluting the Fe^{2+} NS sensor batch by 0.5× and 0.25× stock solutions, both the dynamic and linear range decreased in the colorimetric mode (Figure S13). As expected, in the fluorescence mode, the span of the sensors also decreased proportionally to the dilution factor with the normalized midpoint response (log EC_{50}) also decreasing (Figure S13), thus providing a slight increase in sensitivity.

This nanoscale extraction approach is beneficial for a researcher looking to rapidly quantify a metal of interest. Though this approach follows similar LLE principles, it is specified for sensing and is not all-encompassing to LLE applications. An instance in which researchers need to extract then purify their analyte of interest with chromatography for further analysis is not compatible with our approach because the metal−ligand complex stays encased in the nanoparticle. Another scenario where this method would not work is one in which the researcher needs to separate the two liquid phases after extraction to get rid of optically opaque matrices. In our method, the nanoparticle suspensions are injected directly into the sample, and the measurement is taken on the mixture. For this reason, colored or turbid matrices could significantly interfere with measuring analytes in the colorimetric mode of this approach. While there are analytical procedures to mitigate matrix effects, the fluorescence readout mode is still recommended in these cases as it may enable quantification even in some colored samples. Chemical probe synthesis is a popular area of study;[60] however, there is no probe for every application. The last setting in which this new method would not work is one in which the researcher is attempting to extract an analyte that does not have a ligand that is soluble inside a hydrophobic phase. However, water-soluble probes could be lipophilized to incorporate them into the particle core.

CONCLUSIONS

Here, we introduce a general platform for an alternative phase extraction method for quantifying metal ions. Encapsulating hydrophobic optically responsive ligands inside polymeric nanoparticles enabled successful quantitation of Fe^{2+}, Al^{3+}, and Cu^{+} in aqueous samples. The Fe^{2+} nanosensor response highly correlates to that of a commercial colorimeter, deeming this approach a reliable analytical option. Adopting a polymeric nanoparticle for the extraction matrix provides benefits like a one-step protocol and simple formulation procedures, reduced amounts of organic solvents, higher throughput, fast response times, and the potential for a large expansion of phase extraction applications. Future works will consist of identifying the unwanted, ratiometric response of the Fe^{2+} nanosensors to Cu^{2+}, incorporating optically responsive metal probes for other analytes into the nanoparticles, and applying this nanoparticle extraction assay to samples with highly complex matrices to rapidly measure analytes of interest.

ASSOCIATED CONTENT

Supporting Information

The Supporting Information is available free of charge at https://pubs.acs.org/doi/10.1021/acssensors.1c01780.

(Table S1) Mass components of NS formulations; (Figure S1) filtrate analysis of Fe^{2+}, Al^{3+}, and Cu^{+} NS;

https://doi.org/10.1021/acssensors.1c01780
ACS Sens. 2021, 6, 4408−4416

(Figure S2) linear and nonlinear calibration curves for the Fe^{2+} NS; (Figure S3) absorption spectra showing selectivity of the Fe^{2+} NS with 100 μM, competing metal solutions; (Figure S4) calibration curves for the Fe^{2+} NS with mixed-analyte (Fe^{2+}:Cu^{2+}) standard dilution sets; (Figure S5) comparison of Fe^{2+} standard curve calibration with known Fe^{2+} to standard addition calibration with unknown Fe^{2+}; (Figure S6) fluorescence calibrations that show the functional lifetime of the Fe^{2+} NS; (Figure S7) calibration of Fe^{2+} NS that lack bathophenanthroline against all analytes; (Figure S8) calibrations of the Fe^{2+}, Al^{3+}, and Cu^{+} NS against a fixed analyte and varying pHs; (Figure S9) irreversibility of the Fe^{2+} NS; (Figure S10) fluorescence spectra showing selectivity of the Al^{3+} NS with 100 μM analyte solutions; (Figure S11) absorption spectra of the Cu^{+} NS with increasing concentrations of Cu^{+}; (Figure S12) calibrations of the ratiometric (DiO/DiD) Fe^{2+} NS against competing metals; (Figure S13) calibrations of the diluted Fe^{2+} NS (PDF)

AUTHOR INFORMATION

Corresponding Author

Kevin J. Cash − *Quantitative Biosciences and Engineering and Chemical and Biological Engineering, Colorado School of Mines, Golden, Colorado 80401, United States;* orcid.org/0000-0002-9748-2530; Email: kcash@mines.edu

Authors

Tyler Z. Sodia − *Quantitative Biosciences and Engineering, Colorado School of Mines, Golden, Colorado 80401, United States;* orcid.org/0000-0002-3198-3340

Alexa A. David − *Chemical and Biological Engineering, Colorado School of Mines, Golden, Colorado 80401, United States*

Ashley P. Chesney − *Chemical and Biological Engineering, Colorado School of Mines, Golden, Colorado 80401, United States*

Juliana N. Perri − *Chemical and Biological Engineering, Colorado School of Mines, Golden, Colorado 80401, United States*

Gwendolyn E. Gutierrez − *Green Mountain High School, Lakewood, Colorado 80228, United States*

Cecilia M. Nepple − *Chemical and Biological Engineering, Colorado School of Mines, Golden, Colorado 80401, United States;* orcid.org/0000-0002-8401-0235

Sydney M. Isbell − *Chemical and Biological Engineering, Colorado School of Mines, Golden, Colorado 80401, United States;* orcid.org/0000-0002-1276-6615

Complete contact information is available at: https://pubs.acs.org/10.1021/acssensors.1c01780

Author Contributions

K.J.C. and T.Z.S. conceptualized the study and performed the methodologies; T.Z.S. performed the validation and formal analysis; T.Z.S., A.A.D., A.P.C., J.N.P., G.E.G., C.M.N., and S.M.I. performed the investigation; T.Z.S. performed data curation, wrote the original draft, and performed visualization; K.J.C. and T.Z.S. reviewed and edited the manuscript, supervised the study, and performed project administration; K.J.C. performed funding acquisition.

Notes

The authors declare no competing financial interest.

ACKNOWLEDGMENTS

This material is based upon work supported by the National Science Foundation under Grant No. 1944204. Research reported in this publication was supported by the National Institute of General Medical Sciences of the National Institutes of Health under Award Number R15GM140443. The content is solely the responsibility of the authors and does not necessarily represent the official views of the National Institutes of Health. This work was supported by start-up funds from the Colorado School of Mines. We would like to thank Samuel Saccomano and Adrian Mendonsa for carefully reading and editing the manuscript.

ABBREVIATIONS

LLE, liquid−liquid extraction; NS, nanosensors; BP, bathophenanthroline; 8HQ, 8-hydroxyquinoline; BC, bathocuproine; PNS, polymeric nanosensors; SPE, solid phase extraction

REFERENCES

(1) Carter, K. P.; Young, A. M.; Palmer, A. E. Fluorescent Sensors for Measuring Metal Ions in Living Systems. *Chem. Rev.* **2014**, *114*, 4564−4601.

(2) Zhu, Q.; Aller, R. C. Two-Dimensional Dissolved Ferrous Iron Distributions in Marine Sediments as Revealed by a Novel Planar Optical Sensor. *Mar. Chem.* **2012**, *136-137*, 14−23.

(3) Neu, H. M.; Lee, M.; Pritts, J. D.; Sherman, A. R.; Michel, S. L. J. Seeing the "Unseeable," A Student-Led Activity to Identify Metals in Drinking Water. *J. Chem. Educ.* **2020**, *97*, 3690−3696.

(4) Jackson, B. P.; Punshon, T. Recent Advances in the Measurement of Arsenic, Cadmium, and Mercury in Rice and Other Foods. *Curr. Environ. Health Rep.* **2015**, *2*, 15−24.

(5) Zhu, H.; Fan, J.; Wang, B.; Peng, X. Fluorescent, MRI, and Colorimetric Chemical Sensors for the First-Row d-Block Metal Ions. *Chem. Soc. Rev.* **2015**, *44*, 4337−4366.

(6) Bezerra, M. D. A.; Arruda, M. A. Z.; Ferreira, S. L. C. Cloud Point Extraction as a Procedure of Separation and Pre-Concentration for Metal Determination Using Spectroanalytical Techniques: A Review. *Appl. Spectrosc. Rev.* **2005**, *40*, 269−299.

(7) Standard Methods Online - Standard Methods for the Examination of Water and Wastewater http://standardmethods.org/ (accessed Jul 21, 2021).

(8) Kokosa, J. M. Advances in Solvent-Microextraction Techniques. *TrAC, Trends Anal. Chem.* **2013**, *43*, 2−13.

(9) Constable, E. C.; Housecroft, C. E. The Early Years of 2,2'-Bipyridine-A Ligand in Its Own Lifetime. *Molecules* **2019**, *24*, 3951.

(10) Heaney, S. I.; Davison, W. The Determination of Ferrous Iron in Natural Waters with 2,2′ Bipyridyl. *Limnol. Oceanogr.* **1977**, *22*, 753−760.

(11) Riemer, J.; Hoepken, H. H.; Czerwinska, H.; Robinson, S. R.; Dringen, R. Colorimetric Ferrozine-Based Assay for the Quantitation of Iron in Cultured Cells. *Anal. Biochem.* **2004**, *331*, 370−375.

(12) Seamer, P. A. Estimation of μgm. Quantities of Iron in Culture Medium, using Bathophenanthroline. *Nature* **1959**, *184*, 636−637.

(13) Artiss, J. D.; Vinogradov, S.; Zak, B. Spectrophotometric Study of Several Sensitive Reagents for Serum Iron. *Clin. Biochem.* **1981**, *14*, 311−315.

(14) Lee, G. F.; Stumm, W. Determination of Ferrous Iron in the Presence of Ferric Iron With Bathophenanthroline. *J. AWWA* **1960**, *52*, 1567−1574.

(15) Ghosh, M. M.; O'Connor, J. T.; Engelbrecht, R. S. Bathophenanthroline Method for the Determination of Ferrous Iron. *J. - Am. Water Works Assoc.* **1967**, *59*, 897−905.

(16) Saito, T. Spectrophotometric Determination of Traces of Iron Using a Poly(Vinyl Chloride) Membrane Containing Bathophenanthroline. *Anal. Chim. Acta* **1992**, *268*, 351−355.
(17) Xie, X.; Bakker, E. Ion Selective Optodes: From the Bulk to the Nanoscale. *Anal. Bioanal. Chem.* **2015**, *407*, 3899−3910.
(18) Mistlberger, G.; Crespo, G. A.; Bakker, E. Ionophore-Based Optical Sensors. *Annu. Rev. Anal. Chem.* **2014**, *7*, 483−512.
(19) Du, X.; Xie, X. Ion-Selective Optodes: Alternative Approaches for Simplified Fabrication and Signaling. *Sens. Actuators, B* **2021**, *335*, 129368.
(20) Jewell, M. P.; Greer, M. D.; Dailey, A. L.; Cash, K. J. Triplet-Triplet Annihilation Upconversion Based Nanosensors for Fluorescence Detection of Potassium. *ACS Sensors* **2020**, *5*, 474−480.
(21) Galyean, A. A.; Behr, M. R.; Cash, K. J. Ionophore-Based Optical Nanosensors Incorporating Hydrophobic Carbon Dots and a PH-Sensitive Quencher Dye for Sodium Detection. *Analyst* **2018**, *143*, 458−465.
(22) Ferris, M. S.; Chesney, A. P.; Ryan, B. J.; Ramesh, U.; Panthani, M. G.; Cash, K. J. Silicon Nanocrystals as Signal Transducers in Ionophore-Based Fluorescent Nanosensors. *Sens. Actuators, B* **2021**, *331*, 129350.
(23) Zhai, J.; Xie, X.; Bakker, E. Anion-Exchange Nanospheres as Titration Reagents for Anionic Analytes. *Anal. Chem.* **2015**, *87*, 8347−8352.
(24) Zhai, J.; Xie, X.; Bakker, E. Solvatochromic Dyes as PH-Independent Indicators for Ionophore Nanosphere-Based Complexometric Titrations. *Anal. Chem.* **2015**, *87*, 12318−12323.
(25) Zhai, J.; Bakker, E. Complexometric Titrations: New Reagents and Concepts to Overcome Old Limitations. *Analyst* **2016**, *141*, 4252−4261.
(26) Xie, X.; Zhai, J.; Crespo, G. A.; Bakker, E. Ionophore-Based Ion-Selective Optical NanoSensors Operating in Exhaustive Sensing Mode. *Anal. Chem.* **2014**, *86*, 8770−8775.
(27) Dubach, J. M.; Balaconis, M. K.; Clark, H. A. Fluorescent Nanoparticles for the Measurement of Ion Concentration in Biological Systems. *J. Visualized Exp.* **2011**, *53*, 1−5.
(28) Du, X.; Wang, R.; Zhai, J.; Li, X.; Xie, X. Ionophore-Based Ion-Selective Nanosensors from Brush Block Copolymer Nanodots. *ACS Appl. Nano Mater.* **2020**, *3*, 782−788.
(29) Xie, X.; Mistlberger, G.; Bakker, E. Ultrasmall Fluorescent Ion-Exchanging Nanospheres Containing Selective Ionophores. *Anal. Chem.* **2013**, *85*, 9932−9938.
(30) Moosavi, S. M. *Linearity of Calibration Curves for Analytical Methods: A Review of Criteria for Assessment of Method Reliability*; Stauffer, M., Ed.; IntechOpen: Rijeka, 2018; p Ch. 6. DOI: 10.5772/intechopen.72932.
(31) Harris, D. C. *Quantitative Chemical Analysis*; W. H. Freeman and Company, 2010.
(32) National Center for Biotechnology Information (2021). PubChem Compound Summary for CID 72812, 4,7-Diphenyl-1,10-Phenanthroline. 2021.
(33) Water, Sanitation, H. and H. *Guidelines for Drinking-Water Quality*; 2017.
(34) Wu, L.; Brucker, R. P.; Beard, B. L.; Roden, E. E.; Johnson, C. M. Iron Isotope Characteristics of Hot Springs at Chocolate Pots, Yellowstone National Park. *Astrobiology* **2013**, *13*, 1091−1101.
(35) Espósito, B. P.; Epsztejn, S.; Breuer, W.; Cabantchik, Z. I. A Review of Fluorescence Methods for Assessing Labile Iron in Cells and Biological Fluids. *Anal. Biochem.* **2002**, *304*, 1−18.
(36) Accorsi, G.; Listorti, A.; Yoosaf, K.; Armaroli, N. 1,10-Phenanthrolines: Versatile Building Blocks for Luminescent Molecules, Materials and Metal Complexes. *Chem. Soc. Rev.* **2009**, *38*, 1690−1700.
(37) Kasahara, I.; Ogawa, T.; Hata, N.; Taguchi, S.; Goto, K.; Ohta, M.; Ohzeki, K. Selective and Sensitive Spectrophotometric Determination of Copper in Water after Collection of Its Bathocuproine Complex on an Organic-Solvent-Soluble Membrane Filter. *Water Res.* **1989**, *23*, 933−936.
(38) Agency for Toxic Substances and Disease Registry (ATSDR). Toxicological Profile for Copper. *Dep. Heal. Hum. Serv. Public Heal. Serv.* **2004**.
(39) Fabbrizzi, L.; Licchelli, M.; Pallavicini, P.; Sacchi, D.; Taglietti, A. Sensing of Transition Metals through Fluorescence Quenching or Enhancement. A Review. *Analyst* **1996**, *121*, 1763−1768.
(40) Morgan, B.; Lahav, O. The Effect of PH on the Kinetics of Spontaneous Fe(II) Oxidation by O2 in Aqueous Solution − Basic Principles and a Simple Heuristic Description. *Chemosphere* **2007**, *68*, 2080−2084.
(41) Hirayama, T.; Nagasawa, H. Chemical Tools for Detecting Fe Ions. *J. Clin. Biochem. Nutr.* **2017**, *60*, 39−48.
(42) (2021), N. C. for B. I. PubChem Compound Summary for CID 1923, 8-Hydroxyquinoline.
(43) Yu, G.; Shen, D.; Liu, Y.; Zhu, D. Fluorescence Stability of 8-Hydroxyquinoline Aluminum. *Chem. Phys. Lett.* **2001**, *333*, 207−211.
(44) España, J. S. The Behavior of Iron and Aluminum in Acid Mine Drainage: Speciation, Mineralogy, and Environmental Significance; Letcher Solubility and Environmental Issues. T. M. B. T.-T., Ed.; Elsevier: Amsterdam, 2007, pp. 137−150, DOI: 10.1016/B978-044452707-3/50009-4.
(45) Wei, X.; Viadero, R. C., Jr.; Buzby, K. M. Recovery of Iron and Aluminum from Acid Mine Drainage by Selective Precipitation. *Environ. Eng. Sci.* **2005**, *22*, 745−755.
(46) National Center for Biotechnology Information (2021). PubChem Compound Summary for CID 65149, 2,9-Dimethyl-4,7-Diphenyl-1,10-Phenanthroline.
(47) Müller, E.; Berger, R.; Blass, E.; Sluyts, D.; Pfennig, A. Liquid−Liquid Extraction. *Ullmann's Encycl. Ind. Chem.*. January *15*, 2008. DOI: 10.1002/14356007.b03_06.pub2.
(48) Saito, T. Sensing of Trace Copper Ion by a Solid Phase Extraction-Spectrophotometry Using a Poly(Vinyl Chloride) Membrane Containing Bathocuproine. *Talanta* **1994**, *41*, 811−815.
(49) Martínez, M. V.; Rivarola, C. R.; Miras, M. C.; Barbero, C. A. A Colorimetric Iron Sensor Based on the Partition of Phenanthroline Complexes into Polymeric Hydrogels. Combinatorial Synthesis and High Throughput Screening of the Hydrogel Matrix. *Sens. Actuators, B* **2017**, *241*, 19−32.
(50) Lerchi, M.; Bakker, E.; Rusterholz, B.; Simon, W. Lead-Selective Bulk Optodes Based on Neutral Ionophores with Subnanomolar Detection Limits. *Anal. Chem.*. American Chemical Society,: Washington, DC : 1992, pp. 1534−1540. DOI: 10.1021/ac00038a007.
(51) Lerchi, M.; Reitter, E.; Simon, W.; Pretsch, E.; Chowdhury, D. A.; Kamata, S. Bulk Optodes Based on Neutral Dithiocarbamate Ionophores with High Selectivity and Sensitivity for Silver and Mercury Cations. *Anal. Chem.*. American Chemical Society,: Washington, DC : 1994, pp. 1713−1717. DOI: 10.1021/ac00082a019.
(52) Yamini, Y.; Tamaddon, A. Sensing of Iron Ions by Solid Phase Spectrophotometry. *Iran. J. Chem. Chem. Eng.* **2002**, *21*, 91−96.
(53) Dubach, J. M.; Das, S.; Rosenzweig, A.; Clark, H. A. Visualizing Sodium Dynamics in Isolated Cardiomyocytes Using Fluorescent Nanosensors. *Proc. Natl. Acad. Sci.* **2009**, *106*, 16145.
(54) Jewell, M. P.; Galyean, A. A.; Kirk Harris, J.; Zemanick, E. T.; Cash, K. J. Luminescent Nanosensors for Ratiometric Monitoring of Three-Dimensional Oxygen Gradients in Laboratory and Clinical Pseudomonas Aeruginosa Biofilms. *Appl. Environ. Microbiol.* **2019**, *85*, e01116−e01119.
(55) Cash, K. J.; Clark, H. A. Phosphorescent Nanosensors for in Vivo Tracking of Histamine Levels. *Anal. Chem.* **2013**, *85*, 6312−6318.
(56) Rong, G.; Corrie, S. R.; Clark, H. A. In Vivo Biosensing: Progress and Perspectives. *ACS Sensors* **2017**, *2*, 327−338.
(57) Viñas, P.; Campillo, N.; López-García, I.; Hernández-Córdoba, M. Dispersive Liquid−Liquid Microextraction in Food Analysis. A Critical Review. *Anal. Bioanal. Chem.* **2014**, *406*, 2067−2099.

(58) Ferris, M. S.; Behr, M. R.; Cash, K. J. An Ionophore-Based Persistent Luminescent 'Glow Sensor' for Sodium Detection. *RSC Adv.* **2019**, *9*, 32821−32825.
(59) Doussineau, T.; Schulz, A.; Lapresta-Fernandez, A.; Moro, A.; Körsten, S.; Trupp, S.; Mohr, G. J. On the Design of Fluorescent Ratiometric Nanosensors. *Chem. - Eur. J.* **2010**, *16*, 10290−10299.
(60) Chowdhury, S.; Rooj, B.; Dutta, A.; Mandal, U. Review on Recent Advances in Metal Ions Sensing Using Different Fluorescent Probes. *J. Fluoresc.* **2018**, *28*, 999−1021.

https://doi.org/10.1021/acssensors.1c01780
ACS Sens. 2021, 6, 4408−4416